

Effect of the Pauli Exclusion Principle on the Potential of Nucleus–Nucleus Interaction

V. Yu. Denisov* and V. A. Nesterov

Institute for Nuclear Research, National Academy of Sciences of Ukraine, pr. Nauki 47, 03680, Kyiv, Ukraine

Received July 17, 2009; in final form, December 18, 2009

Abstract—The dependence of the potentials of nucleus–nucleus interaction on taking into account the antisymmetrization of nucleons and the contribution of the nucleon kinetic energy to the potential is studied within approaches based on the energy–density functional, double–folding model, and the two–center shell model. It is shown that the contribution of the nucleon kinetic energy in colliding nuclei leads to the appearance of a significant core at short distances between the nuclei involved.

DOI: 10.1134/S1063778810070070

1. INTRODUCTION

In order to calculate various features of nuclear reactions, it is necessary to know the potential energy of interaction between the nuclei involved, the strength and the radial dependence of the potential of interaction between the nuclei being of paramount importance [1–22].

The energy of interaction between nuclei receives contributions from the Coulomb interaction of protons and from the nuclear interaction of nucleons contained in colliding nuclei. In the case of spherical nuclei, the potential of interaction between them can be represented in the form of the sum of three terms depending only on the distance between the nuclei. These are the Coulomb, nuclear, and rotational components of the potential.

The Coulomb interaction of protons of colliding nuclei is known quite well. However, the interaction between nuclei that is due to nucleon–nucleon forces has received much less adequate study. In view of this, a large number of various approximations have been proposed to date for calculating this component of the nucleus–nucleus interaction [1–22]. One usually specifies the rotational term of the interaction potential in the approximation of pointlike nuclei, and we will not consider it in detail here.

In order to determine the nucleus–nucleus interaction, it is highly desirable to employ the most precise methods that have been developed for describing the energy of nucleus–nucleus interaction, the properties of nuclei, and the properties of nuclear matter. Some of these methods will also be used in the present study pursuing the goal of clarifying the

dependence of the nucleus–nucleus potential on the effect of the Pauli exclusion principle in the set of nucleons of colliding nuclei and the effect of taking into account the kinetic energy of these nucleons on the nucleus–nucleus potential. In particular, we apply the approach of the energy–density functional (namely, the extended Thomas–Fermi method [10, 11, 22–24]) and the two–center shell model [16], as well as the double–folding method [2–5, 20, 21].

We note that, in the extended Thomas–Fermi approximation, the antisymmetrization of nucleons and the Pauli exclusion principle are taken into account directly in calculating the kinetic energy of nucleons, this being accompanied by the emergence of a significant contribution of the kinetic energy of nucleons to the potential. It should also be noted that the importance of the contribution of the kinetic energy of nucleons to the potential of interaction between nuclei was discussed in [14]. The contribution of the kinetic energy of nucleons is neglected, as a rule, in calculating the potential in the double–folding approximation [2–5, 20], but this contribution was taken into account in [15], where a significant change in the momentum distribution of nucleons in colliding nuclei was assumed.

In the present article, we discuss in detail the properties of potentials obtained in various approximations and analyze the effect of the Pauli exclusion principle and of the antisymmetrization of nucleons on the nucleus–nucleus potential.

The ensuing exposition is organized as follows.

In Section 2, we outline various approximations used to calculate nucleus–nucleus interaction. In section 3, we discuss the results obtained by calculating the potentials of nucleus–nucleus interaction

*E-mail: denisov@kinr.kiev.ua

within various approaches. Section 4 presents our conclusions and outlook.

2. POTENTIAL OF NUCLEUS–NUCLEUS INTERACTION

2.1. Approximation of the Energy-Density Functional

In the approximation of the energy-density functional [10, 11, 17, 22–24], the potential of nucleus–nucleus interaction is the difference of the energy of the system of two nuclei at a finite distance, $E_{12}(R)$, and the respective energy at an infinite distance, $E_1 + E_2$; that is,

$$V_{\text{ED}}(R) = E_{12}(R) - E_1 - E_2. \quad (1)$$

One can find the corresponding energy densities, knowing the nucleon-density distributions in nuclei and the energy-density functional in nuclei:

$$E_{12} = \int \varepsilon[\rho_{1p}(\mathbf{r}) + \rho_{2p}(\mathbf{r}, R), \rho_{1n}(\mathbf{r}) + \rho_{2n}(\mathbf{r}, R)] d\mathbf{r}, \quad (2)$$

$$E_1 = \int \varepsilon[\rho_{1p}(\mathbf{r}), \rho_{1n}(\mathbf{r})] d\mathbf{r}, \quad (3)$$

$$E_2 = \int \varepsilon[\rho_{2p}(\mathbf{r}), \rho_{2n}(\mathbf{r})] d\mathbf{r}. \quad (4)$$

Here, ε is the energy-density functional; ρ_{1n} and ρ_{1p} are, respectively, the neutron and the proton density in the first nucleus; ρ_{2n} and ρ_{2p} are the respective nucleon densities in the second nucleus; and R is the distance between the centers of mass of the nuclei.

We note that the energy-density functional contains terms associated with the kinetic and potential energies of nucleons; that is,

$$\begin{aligned} \varepsilon[\rho_p(\mathbf{r}), \rho_n(\mathbf{r})] \\ = \tau[\rho_p(\mathbf{r}), \rho_n(\mathbf{r})] + v[\rho_p(\mathbf{r}), \rho_n(\mathbf{r})]. \end{aligned} \quad (5)$$

Within the approach based on the energy-density functional, we can therefore represent the potential of nucleus–nucleus interaction in the form

$$V_{\text{ED}}(R) = T(R) + V_{\text{pot}}(R), \quad (6)$$

where $T(R)$ and V_{pot} are the contributions of, respectively, the kinetic and potential energies of nucleons to the potential of nucleus–nucleus interaction. These contributions are also related to the nucleon densities in nuclei. Specifically, we have

$$\begin{aligned} T(R) = \int \tau(\rho_{1p} + \rho_{2p}, \rho_{1n} + \rho_{2n}) dV \\ - \int \tau(\rho_{1p}, \rho_{1n}) dV - \int \tau(\rho_{2p}, \rho_{2n}) dV, \end{aligned} \quad (7)$$

$$\begin{aligned} V(R) = \int v(\rho_{1p} + \rho_{2p}, \rho_{1n} + \rho_{2n}) dV \\ - \int v(\rho_{1p}, \rho_{1n}) dV - \int v(\rho_{2p}, \rho_{2n}) dV. \end{aligned} \quad (8)$$

In the present study, we employ Skyrme forces [25], and this makes it possible to obtain explicit expressions for the energy density.

To terms of second order in \hbar , the kinetic-energy density is given by [23]

$$\tau[\rho_p, \rho_n] = \tau_{\text{TF},p} + \tau_{2p} + \tau_{\text{TF},n} + \tau_{2,n}, \quad (9)$$

where

$$\tau_{\text{TF},n(p)} = k\rho_{n(p)}^{5/3} \quad (10)$$

is the density of the kinetic energy of neutrons (protons) in the Thomas–Fermi approximation; $k = \frac{5}{3}(3\pi^2)^{2/3}$; and $\tau_{2n(p)}$ is a gradient correction of second order in \hbar in the nonlocal case [23, 24],

$$\begin{aligned} \tau_{2q} = b_1 \frac{(\nabla\rho_q)^2}{\rho_q} + b_2 \nabla^2\rho_q \\ + b_3 \frac{(\nabla f_q \nabla\rho_q)}{f_q} + b_4 \rho_q \frac{\nabla^2 f_q}{f_q} + b_5 \rho_q \left(\frac{\nabla f_q}{f_q} \right)^2 \\ + b_6 h_m^2 \rho_q \left(\frac{W_q}{f_q} \right)^2. \end{aligned} \quad (11)$$

Here, $b_1 = 1/36$, $b_2 = 1/3$, $b_3 = 1/6$, $b_4 = 1/6$, $b_5 = -1/12$, and $b_6 = 1/2$ are numerical coefficients; $h_m = \hbar^2/(2m)$; $q = p, n$; and the last term in (11) stems from taking into account spin–orbit interaction.

In the case of Skyrme forces, the potential-energy has the form

$$\begin{aligned} \epsilon_{\text{pot}} = \frac{1}{2} t_0 \\ \times \left[\left(1 + \frac{1}{2} x_0 \right) \rho^2 - \left(x_0 + \frac{1}{2} \right) (\rho_n^2 + \rho_p^2) \right] \\ + \frac{1}{12} t_3 \rho^\alpha \left[\left(1 + \frac{1}{2} x_3 \right) \rho^2 - \left(x_3 + \frac{1}{2} \right) (\rho_n^2 + \rho_p^2) \right] \\ + \frac{1}{4} \left[t_1 \left(1 + \frac{1}{2} x_1 \right) + t_2 \left(1 + \frac{1}{2} x_2 \right) \right] \tau \rho \\ + \frac{1}{4} \left[t_2 \left(x_2 + \frac{1}{2} \right) - t_1 \left(x_1 + \frac{1}{2} \right) \right] (\tau_n \rho_n + \tau_p \rho_p) \\ + \frac{1}{16} \left[3t_1 \left(1 + \frac{1}{2} x_1 \right) - t_2 \left(1 + \frac{1}{2} x_2 \right) \right] (\nabla\rho)^2 \\ - \frac{1}{16} \left[3t_1 \left(x_1 + \frac{1}{2} \right) + t_2 \left(x_2 + \frac{1}{2} \right) \right] ((\nabla\rho_p)^2 \\ + (\nabla\rho_n)^2) + \frac{1}{2} W_0 [J\nabla\rho + J_n \nabla\rho_n + J_p \nabla\rho_p]. \end{aligned} \quad (12)$$

Here, $t_0, t_1, t_2, t_3, x_0, x_1, x_2, x_3, \alpha$, and W_0 are the parameters of the Skyrme potential; $\rho = \rho_n + \rho_p$; $\tau = \tau_n + \tau_p$; $J = J_n + J_p$; and

$$f_{n(p)} = 1 + h_m(\alpha + \beta)\rho_{n(p)} + h_m\alpha\rho_{p(n)}, \quad (13)$$

$$\alpha = \frac{1}{4} \left[t_1 \left(1 + \frac{1}{2}x_1 \right) + t_2 \left(1 + \frac{1}{2}x_2 \right) \right], \quad (14)$$

$$\beta = \frac{1}{4} \left[t_2 \left(x_2 + \frac{1}{2} \right) - t_1 \left(x_1 + \frac{1}{2} \right) \right],$$

$$J_{n(p)} = -\frac{h_m}{f_{n(p)}}\rho_{n(p)}\mathbf{W}_{n(p)}, \quad (15)$$

$$\mathbf{W}_{n(p)} = \frac{W_0}{2} [2\nabla\rho_{n(p)} + \nabla\rho_{p(n)}].$$

It should be noted that some terms of the potential-energy density contain the kinetic-energy density, since Skyrme forces are velocity-dependent. Including these terms in the kinetic energy, we obtain a different form of the energy-density functional,

$$\varepsilon_{\text{Skyrme}} = \frac{\hbar^2}{2m^*}\tau + \varepsilon_{\text{pot}}, \quad (16)$$

where m^* is the so-called effective mass and $\varepsilon_{\text{pot}} = \varepsilon_{\text{pot}}|_{\tau=\tau_p=\tau_n=0}$ is the potential energy not involving kinetic-energy terms. Usually, the inequality $m^*/m < 1$ holds for Skyrme forces; therefore, the contribution of the kinetic energy of nucleons to the nucleus–nucleus potential is sizable.

2.2. Double-Folding Method

Potentials obtained on the basis of the double-folding method have been widely used in recent years [1–5, 20, 21]. This method employs the nucleon–nucleon interaction v and the ground-state density distributions $\rho_{1(2)}$ in colliding nuclei; that is,

$$\begin{aligned} & V_{\text{DF}}(R) \\ &= NG(E) \int d\mathbf{r}_1 d\mathbf{r}_2 \rho_1(\mathbf{r}_1) F(\rho_1(\mathbf{r}_1) \\ &+ \rho_2(\mathbf{r}_2)) v(\mathbf{R} + \mathbf{r}_2 - \mathbf{r}_1) \rho_2(\mathbf{r}_2), \end{aligned} \quad (17)$$

where \mathbf{r}_1 and \mathbf{r}_2 are the radius vectors that specify the positions of interacting nucleons in the reference frames comoving with the centers of mass of the nuclei and R is the distance between these centers of mass. The functions $F(\rho)$ and $G(E)$ describe the dependence of the nucleon–nucleon interaction on the nucleon densities and the collision energy, and one usually selects the factor N in such a way as to attain the best description of scattering data. It should be noted that the nucleon-density distributions in interacting nuclei can be obtained within different

approaches and that the forces acting between the nucleons may also be different.

For the potentials obtained on the basis of the double-folding method to lead to a good description of experimental data, additional dependences on the nucleon-distribution density $F(\rho)$ and on the collision energy $G(E)$ were introduced in [20, 21]. Below, we employ modern modifications of the double-folding method and modern sets of interaction parameters. In them, use is made of the *DDM3Y* and *DDM3Y-Raid* nucleon–nucleon forces, which depend on the density distribution in colliding nuclei and on the collision energy. In this case, we have [20]

$$G(E) = 1 - 0.002E, \quad (18)$$

$$F(\rho) = C(1 + \alpha \exp(-\beta\rho)), \quad (19)$$

where E is the collision energy in MeV units; ρ is the nucleon-distribution density; and C, α , and β are parameters that are determined from a fit to data on the scattering on nuclei.

2.3. Double-Folding Model with Allowance for the Kinetic-Energy Contribution

The contribution that is generated by the internal kinetic energy of nucleons and which was taken directly into account in considering the nucleus–nucleus potential in the energy-density approximation [see expression (7)] is discarded within the standard double-folding method, which was described in the preceding section. For this reason, the potentials obtained on the basis of the standard double-folding method [1–5, 20, 21] are very deep. The double-folded potential (17) employs the frozen ground-state densities of colliding nuclei [1, 3–5, 15, 20, 21]. At short distances between the nuclei, the nuclear densities overlap considerably, with the result that the internal kinetic energy of nucleons in colliding nuclei changes substantially because of the Pauli exclusion principle. The contribution of the internal kinetic energy of nucleons for their specific distribution in coordinate space can be calculated in the standard Thomas–Fermi approximation [see expression (10)] or within its extended version as specified by expressions (9)–(11). We note that, in the Thomas–Fermi approximation, one assumes the population of the lowest levels of the system and therefore estimates the minimum value of the kinetic energy for this distribution of the density in coordinate space. As a result, one can determine the potential in the double-folding method with allowance for the contribution of the internal kinetic energy as

$$V_{\text{DF-kin}}(R) = T(R) + V_{\text{DF}}(R), \quad (20)$$

where $T(R)$ is the contribution that is generated by the internal kinetic energy of nucleons and which

is given by expression (7) and $V_{DF}(R)$ is the ordinary double-folded potential described by Eq. (17). We note that the double-folded potential in (17) involves the frozen ground-state densities of colliding nuclei [1, 3–5, 15, 20, 21], whence it follows that, in calculating the contribution of the internal kinetic energy of nucleons in (7) and (18), it is necessary to employ the corresponding frozen densities as well.

It should be noted that, previously, attempts were made in [15] to take into account, within the double-folding method, the contribution of the kinetic energy of nucleons, but, in that study, a significant change in the momentum distribution of nucleons at short distances between the nuclei was assumed for frozen nucleon densities. The contribution of the kinetic energy of nucleons was taken into account in [21] in studying the properties of nuclear matter, but, in subsequent studies of the same authors, the contribution of the kinetic energy of nucleons was disregarded in calculating the nucleus–nucleus interaction.

In calculating the potential in the double-folding approximation, one usually takes velocity-independent nucleon–nucleon forces, in which case the effective nucleon mass m^* coincides with the ordinary nucleon mass m in calculating the internal kinetic energy of nucleons. As a result, the contribution of the kinetic energy of nucleons to the potential proves to be somewhat smaller than that in the above approximation of the energy density for Skyrme forces. However, it is necessary to consider that m^* may differ from m if one employs velocity-dependent nucleon–nucleon forces in calculating the contribution of the kinetic energy of nucleons to the potential.

It should be emphasized that the nucleus–nucleus potentials discussed in Subsections 2.1–2.3 rely on frozen nucleon densities and differ only by the choice of nucleon–nucleon forces and the contribution of the kinetic energy of nucleons to the potential.

2.4. Two-Center Shell Model

In calculating the nucleus–nucleus potential, use is also made of models based on the idea of the shell structure of the nucleus. As an example, we can indicate the two-center shell model [16] employing Skyrme forces. In that case, the nucleus–nucleus potential is also determined by relations (1)–(4) with the nucleon-distribution density found for each distance between the nuclei within the two-center shell model. The direct inclusion of the Pauli exclusion principle and of the antisymmetrization of nucleons contained in colliding nuclei is an advantage of this model.

It should be noted that, in contrast to the nucleus–nucleus potentials considered in the preceding sections and associated with frozen densities of nuclei,

the potential calculated within the two-center shell model is determined with allowance for nucleon densities that are characteristic of a specific distance between the nuclei. The potential calculated within the two-center shell model corresponds to slow collisions, in which case the nucleon density has time to undergo relaxation for each distance between the nuclei. Therefore, this potential is adiabatic. In contrast to this, the potentials considered in the preceding sections are associated with frozen nucleon densities and can be applied under conditions of fast collisions, in which case the nucleon density in nuclei does not have time to change significantly within the collision time.

3. NUCLEAR PARTS OF POTENTIALS OF INTERACTION BETWEEN NUCLEI

In [22], we studied in detail the dependence of the nuclear part of the potential of interaction between nuclei in the vicinity of the barrier on the diffuseness of the nucleon-density distribution in nuclei within the approach of the energy-density functional. In the present study, we focus on considering the dependence of a general potential of nucleus–nucleus interaction on the choice of the nucleon-density distribution and method for constructing potentials. The consideration is performed entirely for the example of the potential of interaction between two ^{16}O nuclei.

3.1. Nucleon-Density Distribution

For the proton densities, we have employed the experimental charge densities [26], as well as the proton-density distributions obtained in the Hartree–Fock approximation, by the extended Thomas–Fermi method with allowance for the expansion of the kinetic-energy density to terms of order \hbar^2 , and on the basis of the shell model. The theoretical nucleon distributions used here were obtained on the basis of density-dependent Skyrme forces—in particular, in the SkM^* parametrization [23].

Figure 1a displays the nucleon densities obtained in various approximations. We note that the densities obtained in the Hartree–Fock approximation and especially on the basis of the shell model have a dip at the center of the nucleus. A decrease in the density at the center of the nucleus is associated with shell effects, which are absent in the other densities. The nucleon-density distribution determined within the extended Thomas–Fermi method is characterized by a faster decrease in the diffuse region.

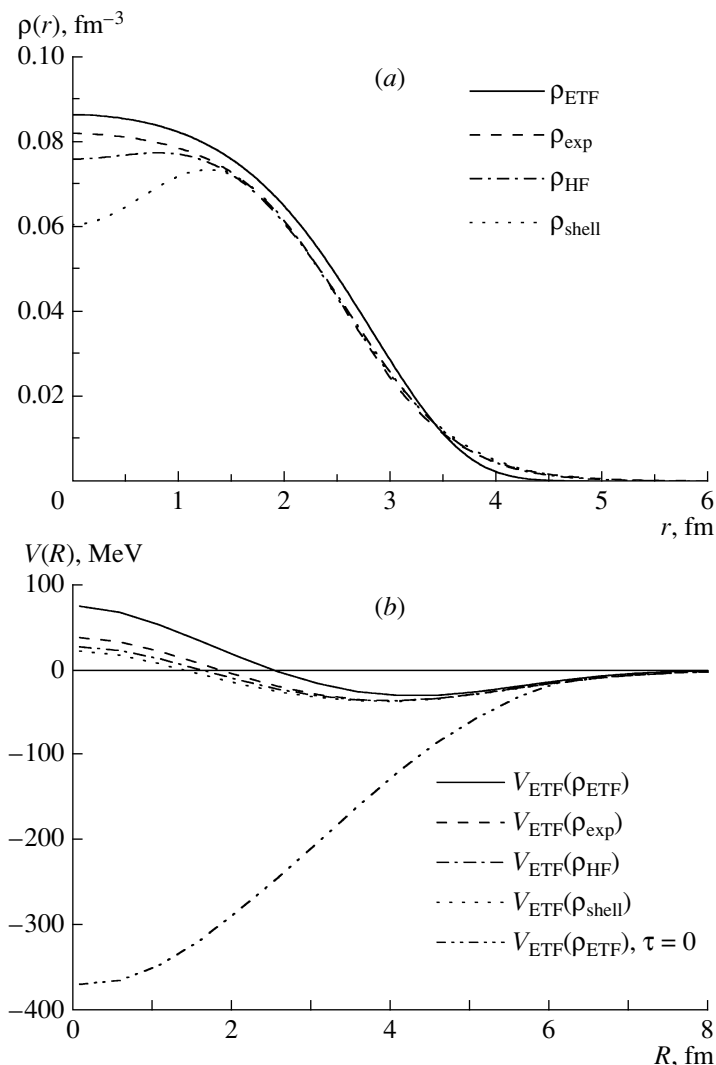


Fig. 1. (a) Nucleon-density distributions for the ^{16}O nucleus that were obtained by the extended Thomas–Fermi method (ρ_{ETF}), experimentally (ρ_{exp} [7]), by the Hartree–Fock method (ρ_{HF}), and on the basis of the shell model (ρ_{shell}); (b) ^{16}O – ^{16}O interaction potentials $V_{\text{ETF}}(\rho_{\text{ETF}})$, $V_{\text{ETF}}(\rho_{\text{exp}})$, $V_{\text{ETF}}(\rho_{\text{HF}})$, and $V_{\text{ETF}}(\rho_{\text{shell}})$ calculated within the method of the energy-density functional by using the nucleon densities presented in Fig. 1a with allowance for the kinetic-energy contribution, the potential $V_{\text{ETF}}(\rho_{\text{ETF}}, \tau = 0)$ being calculated with the nucleon-density distribution obtained by the extended Thomas–Fermi method without allowance for the kinetic-energy contribution ($\tau_p = \tau_n = \tau = 0$).

3.2. Potential of Nucleus–Nucleus Interaction within the Approach of the Energy-Density Functional

The calculation of the potential in the approximation of the energy density functional was performed on the basis of the proton and neutron densities obtained in the Hartree–Fock approximation and by the extended Thomas–Fermi method with allowance for the expansion of the kinetic-energy density to terms of order \hbar^2 , as well as on the basis of the shell model (these densities are displayed in Fig. 1a). In employing experimental charge densities [26], we assumed that the neutron density in the ^{16}O nucleus is identical to the proton density. The nucleus–nucleus po-

tential was calculated in the approximation of frozen nucleon densities.

The dependence of the nuclear part of the interaction between two ^{16}O nuclei on the choice of nucleon distribution in them within the method of the energy-density functional is illustrated in Fig. 1b. At long distances, the potential decreases, fast, while, as the distance decreases there arises attraction between the nuclei, but it gives way to a strong repulsion at short distances (core).

The potential depends greatly on special features of the behavior of the densities. For example, the strength of repulsion at short distances depends on

the nucleon-density distribution used in the calculations and on the values of the density at $r = 0$. This is because the density-dependent Skyrme forces involve a term that is proportional to the parameter t_3 , which is dependent on the density distribution, and which leads to the repulsion of nucleons upon an overly strong increase in the density. Moreover, the contribution of the internal kinetic energy of nucleons to the potential increases sharply because of the Pauli exclusion principle and because of a significant increase in the density. The greater the nucleon-density distribution in the central region of the nucleus (at small r), the greater the value of the potential at short distances R between the nuclei. We have performed a calculation that proved to be indicative of the importance of taking into account the internal kinetic energy of nucleons in calculating the potential of nucleus–nucleus interaction. By way of example, Fig. 2b shows the nucleus–nucleus interaction potential $V_{\text{DF-kin}}(\rho_{\text{ETF}})$ calculated with the nucleon density obtained by the extended Thomas–Fermi method but without including the kinetic energy of nucleons—this is the case of $\tau_p = \tau_n = \tau = 0$. Without allowance for the kinetic energy of nucleons, the repulsive core at small R disappears, and the potential becomes attractive and very deep.

3.3. Potential of Nucleus–Nucleus Interaction in the Double-Folding Approximation

Within the double-folding method, the nuclear part of the potential for the $^{16}\text{O} + ^{16}\text{O}$ system was calculated by using the collision-energy-dependent parametrizations DDM3Y (Fig. 2a) and DDM3Y-Raid (Fig. 2b) of nucleon forces. These calculations were performed at the collision energy of $E = 250$ MeV. In order to simplify the figures, we took the nucleon-density distribution obtained previously in the Hartree–Fock approximation and the extended Thomas–Fermi approximation (see Fig. 1a).

The nucleus–nucleus interaction potentials $V_{\text{DF}}(R)$ depicted in Fig. 2 depend only slightly on the details of the behavior of the nucleon densities, but they depend strongly on the choice of nucleon–nucleon interaction, the same pattern being observed at different energy values. The resulting potentials appear to be deep at short distances. The depths of double-folded potentials $V_{\text{DF}}(R)$ are on the same order of magnitude as the depths of potentials calculated in the extended Thomas–Fermi approximation without taking into account the kinetic-energy contribution ($\tau_p = \tau_n = \tau = 0$)—see Figs. 1b and 2b. The introduction of an explicit density dependence in the potential (DDM3Y forces) reduces substantially the depth of the potential.

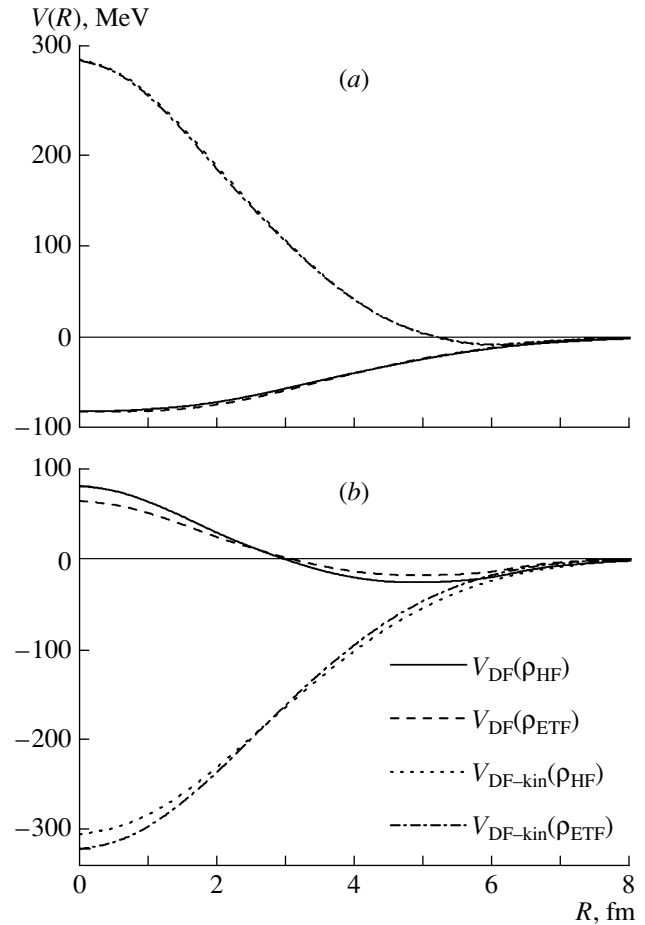


Fig. 2. Double-folded potentials calculated for (a) DDM3Y-Raid and (b) DDM3Y forces by using the nucleon densities obtained by using the extended Thomas–Fermi method [$V_{\text{DF}}(\rho_{\text{ETF}})$ and $V_{\text{DF-kin}}(\rho_{\text{ETF}})$] and by the Hartree–Fock method [$V_{\text{DF}}(\rho_{\text{HF}})$ and $V_{\text{DF-kin}}(\rho_{\text{HF}})$]. The potentials $V_{\text{DF}}(\rho_{\text{ETF}})$ and $V_{\text{DF}}(\rho_{\text{HF}})$ were obtained with allowance for the kinetic-energy contribution, while the potentials $V_{\text{DF-kin}}(\rho_{\text{ETF}})$ and $V_{\text{DF-kin}}(\rho_{\text{HF}})$ were calculated without this contribution ($\tau_p = \tau_n = \tau = 0$).

The contribution of the internal kinetic energy of nucleons to the nucleus–nucleus potential [see Eq. (20)] changes drastically the double-folded potential, which transforms from an attractive potential $V_{\text{DF}}(R)$ into the repulsive potential $V_{\text{DF-kin}}(R)$ at short distances (see Fig. 2). We note that effective nucleon–nucleon forces used to calculate the potential within the double-folding model do not feature a velocity dependence like that in Skyrme forces; therefore, the effective mass proves to be equal to the nucleon mass. This leads to a somewhat smaller kinetic-energy-contribution-induced variation of the potential at short distances between the nuclei than that in the case of Skyrme forces.

The magnitude of the core in the potentials, $V_{\text{DF-kin}}(R)$, depends on the choice of nucleon–

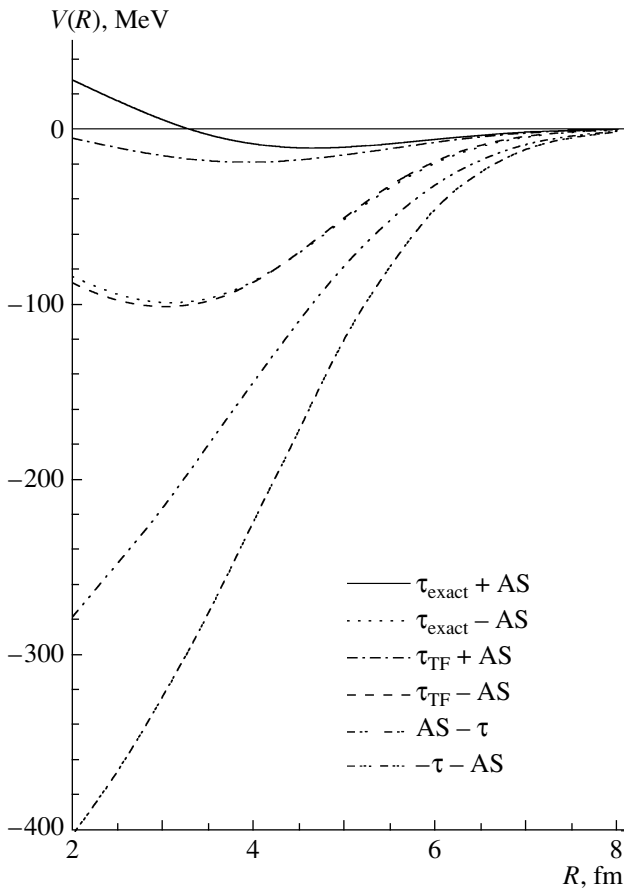


Fig. 3. Potential of interaction in the $^{16}\text{O} + ^{16}\text{O}$ system according to calculations on the basis of the two-center shell model (solid curve) in the case of taking precisely into account the kinetic energy and performing a complete antisymmetrization of nucleons ($\tau_{\text{exact}} + \text{AS}$), (dotted curve) with a precise value of the kinetic energy but without taking into account antisymmetrization ($\tau_{\text{exact}} - \text{AS}$), (dash-and-dot curve) with the kinetic energy in the Thomas–Fermi approximation but with allowance for antisymmetrization ($\tau_{\text{TF}} + \text{AS}$), (dashed curve) with the kinetic energy in the Thomas–Fermi approximation and without allowance for antisymmetrization ($\tau_{\text{TF}} - \text{AS}$), (dash-and-double-dot curve) with allowance for antisymmetrization but without the kinetic-energy contribution ($\text{AS} - \tau$), and (dash-and-triple-dot curve) without antisymmetrization and without the kinetic-energy contribution ($-\tau - \text{AS}$).

nucleon forces. For example, the potentials $V_{\text{DF-kin}}(R)$ calculated with DDM3Y forces are close to the potentials found with Skyrme forces, as one can see from a comparison of Figs. 1 and 2.

3.4. Potential of Nucleus–Nucleus Interaction in the Two-Center Shell Model

The potential obtained for the nuclear part of the interaction for the $^{16}\text{O} + ^{16}\text{O}$ system within the two-center shell model is also of interest. In this case,

32 nucleons of colliding nuclei populate the lowest single-particle levels in two wells of harmonic-oscillator potentials centered at the points whose coordinates are $R/2$ and $-R/2$. The system being considered has a cylindrical symmetry and depends on the coordinates z and ρ . Here, the density distribution in space depends substantially on R . In this case, the potential is adiabatic, in contrast to the potentials considered above, which are based on frozen nucleon densities. For parameters specifying the potential, we take R and k . In the c.m. frame, the nuclei then move at the momenta $k \cdot A$ and $-k \cdot A$, where A is the number of particles. As in [16], we set $k = 0$ in order to simplify the calculations. The nucleon density was calculated on the basis of the shell model in two approximations—that is, with and without allowance for the antisymmetrization of nucleons in colliding nuclei. Moreover, the kinetic energy of nucleons in colliding nuclei was calculated either precisely or in the Thomas–Fermi approximation. The results obtained by calculating the potential for the nuclear part of the interaction for the $^{16}\text{O} + ^{16}\text{O}$ system on the basis of various versions of calculations within the two-center shell model are displayed in Fig. 3.

Comparing the curves in Fig. 3, we can draw the following conclusions:

(i) At long distances, the potential depends only slightly on the approximation in which one calculates the kinetic energy (precise quantum-mechanical calculation versus the Thomas–Fermi approximation), but, at short distances between colliding nuclei, the kinetic energy obtained in the Thomas–Fermi approximation proves to be smaller than that found in a precise quantum-mechanical calculation.

(ii) Allowance for the antisymmetrization of nucleons in colliding nuclei is of importance for determining the potential, since the potential appears to be much deeper if one disregards antisymmetrization.

(iii) The potential calculated with allowance for the contribution of the internal kinetic energy of nucleons and their antisymmetrization at short distances has a repulsive core, whereas the potential calculated without allowance for the internal kinetic energy of nucleons does not have a core at short distances and is strongly attractive.

Figures 4 and 5 show, respectively, the nucleon-density distribution and the kinetic-energy distribution for the system consisting of two ^{16}O nuclei. These distributions were calculated for the distances of 1, 2, and 3 fm between colliding nuclei (upper, middle, lower panels, respectively in Figs. 4 and 5). The distributions in the left-handed panels of Figs. 4 and 5 were obtained in the approximation of frozen nucleon densities determined on the basis of the shell

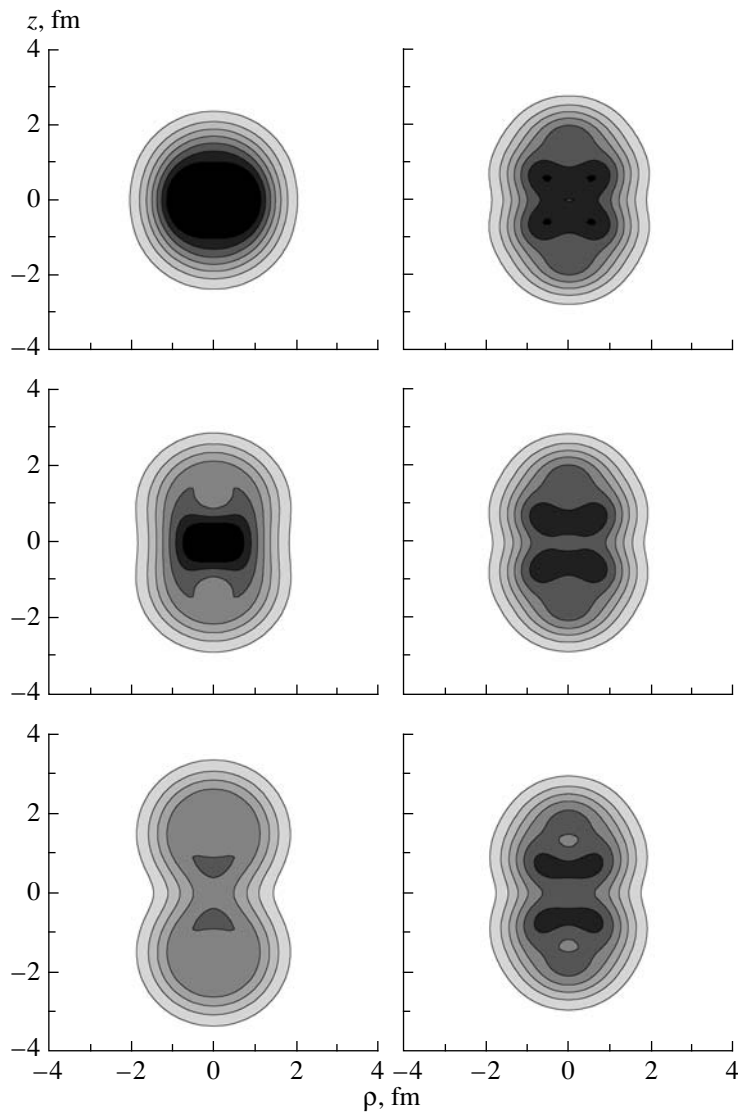


Fig. 4. Behavior of the nucleon-density distribution in the $^{16}\text{O} + ^{16}\text{O}$ system at distances of 1 (upper panels), 2 (middle panels), and 3 fm (lower panels) without (left-hand panels) and with (right-hand panels) allowance for antisymmetrization. The step between the density isolines is 0.02 fm^{-3} .

model for each nucleus individually (see also the corresponding density distributions in Fig. 1). The distributions in the right-hand panels were determined for the densities calculated within the two-center model with allowance for the antisymmetrization of nucleons in colliding nuclei. The kinetic-energy densities in the left-hand panels of Fig. 5 were calculated in the Thomas–Fermi approximation with frozen nucleon densities, while the respective distributions in the right-hand panels were found on the basis of the exact quantum-mechanical expression for the kinetic energy with allowance for antisymmetrization and the Pauli exclusion principle for nucleon densities.

Comparing the nucleon-density distributions and the kinetic-energy distribution in Figs. 4 and 5, we

can see that the nucleon-density distributions found in the two approximations in question differ substantially from each other. Thus, the densities in the instantaneous approximation are more compact in space and, at short distances, exceed considerably the equilibrium density in the region where the nuclei being considered overlap significantly. The antisymmetrization of nucleons naturally leads to their redistribution in space, the maximum densities of the nucleon and kinetic-energy distributions being smaller even at short distances than the corresponding maximum densities calculated in the frozen-density distribution. The kinetic-energy densities are modified considerably upon antisymmetrization. For example, the distribution of the kinetic-energy density becomes

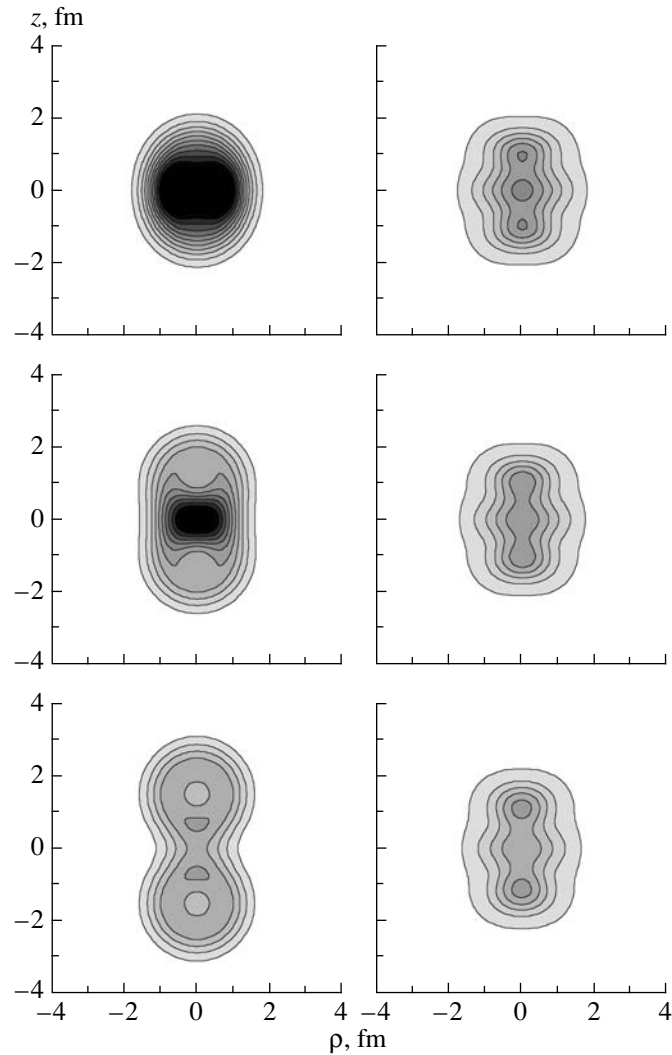


Fig. 5. Behavior of the kinetic-energy-density distribution for the $^{16}\text{O} + ^{16}\text{O}$ system at distances of 1 (upper panels), 2 (middle panels), and 3 fm (lower panels) calculated either within the Thomas–Fermi approach (left-hand panels) or by the exact formula (right-hand panels). The step between the respective isolines is 0.05 MeV fm^{-3} .

more compact in space and smaller in amplitude. As a result, the repulsion between the nuclei at short distances that was calculated in the approximation of frozen densities is stronger than its counterpart determined in the approximation of the two-center shell model with allowance for antisymmetrization and the Pauli exclusion principle.

4. CONCLUSIONS

Thus, we have considered various approaches to constructing nucleus–nucleus potentials, paying particular attention to the contributions of the internal kinetic energy of nucleons and their antisymmetrization to the nucleus–nucleus potential. Comparing the potentials obtained within different approaches, we have arrived at the conclusion that, in order to

construct a realistic potential of nucleus–nucleus interaction, one must calculate it, taking into account both the antisymmetrization of nucleons and their internal kinetic energy.

Although the interaction potential for the $^{16}\text{O} + ^{16}\text{O}$ system was constructed most precisely on the basis of the two-center shell model, the application of this method to heavier nuclear systems would involve difficulties. In this connection, we would like to note a realistic behavior of the potential obtained in the extended Thomas–Fermi approximation or the potential obtained by the double-folding method with allowance for the kinetic-energy contribution. In order to describe reaction cross sections with the aid of these potentials, it is necessary to introduce the dependence of the nucleon-density distribution on the energy of colliding nuclei.

We have shown that the inclusion of the kinetic-energy contribution within various approaches leads to the appearance of a repulsive core in the nuclear part of the potential at short distances. In [27], the effect of a repulsive core on cross sections for nuclear reactions was analyzed within a phenomenological approach, and it was indicated there that the contribution of the core to the angular distribution for the elastic scattering of nuclei is quite sizable.

REFERENCES

1. P. E. Hodgson, *Nuclear Heavy-Ion Reactions* (Clarendon, Oxford, 1978).
2. G. R. Satchler and W. G. Love, *Phys. Rep.* **55**, 183 (1979).
3. R. Bass, *Nuclear Reactions with Heavy Ions* (Springer, Berlin, 1980).
4. G. R. Satchler, *Direct Nuclear Reactions* (Clarendon, Oxford, 1983).
5. P. Fröbrich and R. Lipperheide, *Theory of Nuclear Reactions* (Clarendon, Oxford, 1996).
6. J. Blocki et al., *Ann. Phys. (N.Y.)* **105**, 427 (1977).
7. W. D. Myers and W. J. Swiatecki, *Phys. Rev. C* **62**, 044610 (2000).
8. H. J. Krappe, J. R. Nix, and A. J. Sierk, *Phys. Rev. C* **20**, 992 (1979).
9. A. Winther, *Nucl. Phys. A* **594**, 203 (1995).
10. V. Yu. Denisov, *Phys. Lett. B* **526**, 315 (2002).
11. V. Yu. Denisov and W. Nörenberg, *Eur. Phys. J. A* **15**, 375 (2002); V. Yu. Denisov, *Eur. Phys. J. A* **25** (Suppl. 1), 619 (2005).
12. V. I. Kukulin, V. G. Neudatchin, and Yu. F. Smirnov, *Fiz. Élem. Chastits At. Yadra* **10**, 1236 (1979) [*Sov. J. Part. Nucl.* **10**, 492 (1979)].
13. D. T. Khoa and O. M. Knyaz'kov, *Fiz. Élem. Chastits At. Yadra* **21**, 1456 (1990) [*Sov. J. Part. Nucl.* **21**, 623 (1990)].
14. T. Fliessbach, *Z. Phys.* **247**, 117 (1971).
15. V. B. Soubbotin et al., *Phys. Rev. C* **64**, 014601 (2001).
16. D. Brink and F. Stancu, *Nucl. Phys. A* **243**, 175 (1975).
17. K. A. Brueckner, J. R. Buchler, and M. M. Kelly, *Phys. Rev.* **173**, 944 (1968).
18. C. Ngo, B. Tamain, J. Galin, et al., *Nucl. Phys. A* **240**, 353 (1975).
19. H. Ngo and C. Ngo, *Nucl. Phys. A* **348**, 140 (1980).
20. Dao T. Khoa, W. von Oertzen, and H. G. Bohlen, *Phys. Rev. C* **49**, 1652 (1994).
21. Dao T. Khoa and W. von Oertzen, *Phys. Lett. B* **304**, 8 (1993).
22. V. Yu. Denisov and V. A. Nesterov, *Yad. Fiz.* **69**, 1507 (2006) [*Phys. At. Nucl.* **69**, 1472 (2006)].
23. M. Brack, C. Guet, and H.-B. Hakansson, *Phys. Rep.* **123**, 275 (1985).
24. M. Brack and R. K. Bhaduri, *Semiclassical Physics* (Addison-Wesley, New York, 1997).
25. T. H. R. Skyrme, *Nucl. Phys.* **9**, 615 (1959).
26. H. de Vries, C. W. de Jager, and C. de Vries, *At. Data Nucl. Data Tables* **36**, 495 (1987).
27. V. Yu. Denisov and O. I. Davidovskaya, in *Proc. of the Intern. Conf. on Current Problems in Nuclear Physics and Atomic Energy, Kiev, 9–15 June, 2008* (Inst. for Nucl. Res., Kiev, 2009), p. 192; V. Yu. Denisov and O. I. Davidovskaya, *Yad. Fiz.* **73**, 429 (2010) [*Phys. At. Nucl.* **73**, 404 (2010)]; V. Yu. Denisov and O. I. Davidovskaya, *Izv. Akad. Nauk, Ser. Fiz.* (in press).

Translated by A. Isaakyan